18-HEPE, an n-3 fatty acid metabolite released by macrophages, prevents pressure overload–induced maladaptive cardiac remodeling

Jin Endo,[1,2,3] Motoaki Sano,[3] Yosuke Isobe,[1,2] Keiichi Fukuda,[3] Jing X. Kang,[4] Hiroyuki Arai,[1] and Makoto Arita[1,2,5]

[1]Department of Health Chemistry, Graduate School of Pharmaceutical Sciences, the University of Tokyo, 7-3-1 Hongo, Bunkyo-ku, Tokyo 113-0033, Japan
[2]Laboratory for Metabolomics, RIKEN Center for Integrative Medical Sciences (IMS), 1-7-22 Suehiro-cho, Tsurumi-ku, Yokohama, Kanagawa 230-0045, Japan
[3]Department of Cardiology, Keio University School of Medicine, 35 Shinanomachi, Shinjuku-ku, Tokyo 160-8582, Japan
[4]Laboratory for Lipid Medicine and Technology, Massachusetts General Hospital and Harvard Medical School, Boston, MA 02115
[5]PRESTO, Japan Science and Technology Agency, 4-1-8 Honcho, Kawaguchi, Saitama 332-0012, Japan

N–3 polyunsaturated fatty acids (PUFAs) have potential cardiovascular benefit, although the mechanisms underlying this effect remain poorly understood. Fat–1 transgenic mice expressing *Caenorhabditis elegans* n–3 fatty acid desaturase, which is capable of producing n–3 PUFAs from n–6 PUFAs, exhibited resistance to pressure overload–induced inflammation and fibrosis, as well as reduced cardiac function. Lipidomic analysis revealed selective enrichment of eicosapentaenoic acid (EPA) in fat–1 transgenic bone marrow (BM) cells and EPA–metabolite 18–hydroxyeicosapentaenoic acid (18–HEPE) in fat–1 transgenic macrophages. BM transplantation experiments revealed that fat–1 transgenic BM cells, but not fat–1 transgenic cardiac cells, contributed to the antiremodeling effect and that the 18–HEPE–rich milieu in the fat–1 transgenic heart was generated by BM-derived cells, most likely macrophages. 18–HEPE inhibited macrophage-mediated proinflammatory activation of cardiac fibroblasts in culture, and in vivo administration of 18–HEPE reproduced the fat–1 mice phenotype, including resistance to pressure overload–induced maladaptive cardiac remodeling.

CORRESPONDENCE
Makoto Arita:
makoto.arita@riken.jp

Abbreviations used: 12-HETE, 12-hydroxyeicosatetraenoic acid; 18-HEPE, 18-hydroxyeicosapentaenoic acid; AA, arachidonic acid; DHA, docosahexaenoic acid; DPA, docosapentaenoic acid; EPA, eicosapentaenoic acid; GC-MS, gas chromatography mass spectrometry; LC-MS/MS, liquid chromatography tandem mass spectrometry; PGE2, prostaglandin E2; RvE1, resolvin E1; TAC, transverse aortic constriction; TXB2, thromboxane B2.

The beneficial effects of n-3 polyunsaturated fatty acids (PUFAs), primarily eicosapentaenoic acid (EPA) and docosahexaenoic acid (DHA), were first recognized in the late 1960s with epidemiological evidence of the Inuit population, who consumed an n-3 PUFA-rich diet, having a low incidence of myocardial infarction (Mozaffarian and Wu, 2011). Subsequently, large-scale randomized clinical trials confirmed that dietary supplementation of n-3 PUFAs prevented cardiovascular events in patients with recent myocardial infarction (Yokoyama et al., 2007), reduced mortality in patients with symptomatic chronic heart failure who were receiving standard treatment (Tavazzi et al., 2008), and ameliorated left ventricular (LV) functional capacity and decreased the circulating concentrations of inflammatory cytokines such as TNF, IL-1β, and IL-6 in nonischemic dilated cardiomyopathy (Nodari et al., 2011).

Increased cardiac afterload caused by hypertension, aortic valve stenosis, or natural aging is responsible for the pathogenesis and progression of heart failure accompanied by common histological changes, the so-called maladaptive cardiac remodeling (Opie et al., 2006). Sustained pressure overload elicits cardiomyocyte hypertrophy, inflammatory cell infiltration, and fibrosis, thereby changing LV stiffness and geometry (Wynn and Ramalingam, 2012; Weber et al., 2013). The n-3 PUFAs have potential anti-inflammatory activity in a variety of inflammatory diseases, including atherosclerosis, diabetes, asthma and arthritis (Fritsche, 2006; Zhang and Spite, 2012).

The Rockefeller University Press $30.00
J. Exp. Med. 2014 Vol. 211 No. 8 1673-1687
www.jem.org/cgi/doi/10.1084/jem.20132011

1673

Thus, beneficial antiremodeling effects of n–3 PUFAs in the setting of chronic heart failure can be explained by the anti-inflammatory activity, although the mechanisms underlying such effects are poorly understood.

Mammals cannot naturally produce n–3 fatty acids, so they must rely on a dietary supply. Recently, Kang et al. (2004) developed a transgenic mouse expressing the *C. elegans fat-1* gene encoding n–3 desaturase, which converts n–6 to n–3 PUFAs. These fat-1 mice show enrichment of n–3 PUFAs in almost all organs and tissues, and display a resistant phenotype against inflammatory diseases including colitis (Hudert et al., 2006), pancreatitis (Weylandt et al., 2008), osteoarthritis (Huang et al., 2012), atherosclerosis (Wan et al., 2010), obesity-linked insulin resistance (White et al., 2010), and some kinds of cancer (Xia et al., 2006; Weylandt et al., 2011).

In this study, we investigated the effect of expressing the *C. elegans fat-1* transgene on pressure overload–induced cardiac remodeling. The results demonstrated that fat-1 mice are protected from cardiac remodeling in this model, and that this effect is conferred by BM-derived cells. We further demonstrated that 18-HEPE, which was found at higher levels in macrophages from fat-1 mice, inhibits proinflammatory activation of cardiac fibroblasts and that in vivo administration of 18-HEPE reproduces the fat-1 phenotype on pressure overload–induced cardiac remodeling.

RESULTS

Preserved LV function and less fibrosis in fat–1 mice under pressure overload

To examine the impact of elevated tissue n–3 PUFA levels in the setting of maladaptive cardiac remodeling, we subjected both fat-1 transgenic mice and WT mice to pressure overload by transverse aortic constriction (TAC). The pressure overload–induced increase in the heart weight (HW)/body weight (BW) ratio was reduced in fat-1 mice compared with WT mice at 4 wk after TAC (Fig. 1 A). Echocardiographic analysis of cardiac function revealed that the pressure overload–induced decline in percentage fractional shortening (%FS) observed in the WT mice was also significantly alleviated in fat-1 mice at 4 wk after TAC (Fig. 1 B), as was the increase in Nppa and Nppb expressions (Fig. 1 C), whereas measurement of the cardiomyocyte surface area demonstrated similar levels of cardiomyocyte hypertrophy between fat-1 mice and WT mice after TAC (Fig. 1 D). Pressure overload–induced perivascular and interstitial fibrosis were also less in fat-1 mice compared with WT mice (Fig. 1 E). TAC induces the differentiation of cardiac fibroblasts into myofibroblasts, as characterized by the expression of α-smooth muscle actin (α-SMA). In this study, immunohistochemical analysis revealed fewer α-SMA–positive cells in the fibrotic area apparent in TAC-operated fat-1 transgenic hearts compared with that area in the TAC-operated WT hearts (Fig. 1 F), and consistent with this, the pressure overload–induced increase in the expressions of Col1a1, Col3a1, and Tgfb1 was less in fat-1 mice compared with WT mice (Fig. 1 G). These findings indicated that fat-1 mice showed less fibroblast

activation upon pressure overload than WT mice, leading to preservation of %FS.

Myofibroblast activation by pressure overload in turn induces the production of inflammatory cytokines and chemokines (Koyanagi et al., 2000; Kuwahara et al., 2004; Ma et al., 2012). Accordingly, the increased expression of Ccl2, Ccl3, Ccl5, Il6, and Cx3cl1 after TAC in this study was blunted in fat-1 mice compared with WT mice (Fig. 2 A).

Flow cytometric analysis of the temporal dynamics in the number and distribution of inflammatory cells revealed a gradual increase in leukocyte numbers in the heart after TAC that remained elevated for at least 60 d. The majority (76.4 ± 7.6%) of leukocytes at 4 wk after TAC were CD11b^{+} F4/80^{+} macrophages (Fig. 2 B). However, the hearts of fat-1 mice showed fewer CD11b^{+} F4/80^{+} macrophages at 4 wk after TAC than those of WT mice (Fig. 2 C). Consistent with this, immunostaining demonstrated lower numbers of Mac2-positive macrophages in the fibrotic areas of TAC-operated fat-1 mice compared with TAC-operated WT mice (Fig. 2 D).

BM–derived cells, but not cardiac cells, are crucial for cardioprotection under pressure overload

To address which cells are responsible for the antifibrotic fat-1 phenotype, we prepared four chimeric mice by BM transplantation (BMT): WT mice transplanted with WT BM (WT → WT), WT mice transplanted with fat-1 transgenic BM (fat-1 → WT), fat-1 mice transplanted with WT BM (WT → fat-1), and fat-1 mice transplanted with fat-1 transgenic BM (fat-1 → fat-1). We then subjected these BMT chimera mice to pressure overload by TAC.

The pressure overload–induced reduction in %FS was comparable between WT → WT and WT → fat-1 chimera mice, whereas %FS was preserved in fat-1 → WT chimera mice to the same levels as in fat-1 → fat-1 chimera mice (Fig. 3 A). There was less cardiac fibrosis and fewer myocardial macrophages in the fat-1 → WT and fat-1 → fat-1 chimera mice compared with the WT → WT and WT → fat-1 chimera mice (Fig. 3 B). However, cardiomyocyte hypertrophy induced by the pressure overload was similar among the four BMT chimera mice (Fig. 3 C). Consistent with this, the pressure overload–induced up-regulation of *Nppa*, *Col1a1*, *Tgfb1*, *Cx3cl1*, and *Emr1* was also less in the fat-1 → WT and fat-1 → fat-1 chimera mice compared with the other two chimeras (Fig. 3 D).

To visualize BM-derived cells, we prepared three additional mouse chimeras: WT mice transplanted with GFP transgenic mice BM (WT/GFP → WT), WT mice transplanted with fat-1/GFP double-transgenic mice BM (fat-1/GFP → WT), and fat-1 mice transplanted with GFP transgenic mice BM (WT/GFP → fat-1). The reconstitution of BM cells among these three chimeras showed equivalently high efficiency (WT/GFP → WT; 92.98 ± 0.44%, fat-1/GFP → WT; 92.30 ± 1.36%, WT/GFP → fat-1; 92.00 ± 1.03%). Histological analysis of hearts revealed equal numbers of BM-derived GFP^{+} cells in WT/GFP → WT and fat-1/GFP → WT mice before the TAC operation. BM-derived GFP^{+} cells increased in the hearts of all mice at 4 wk after TAC; however, BM-derived
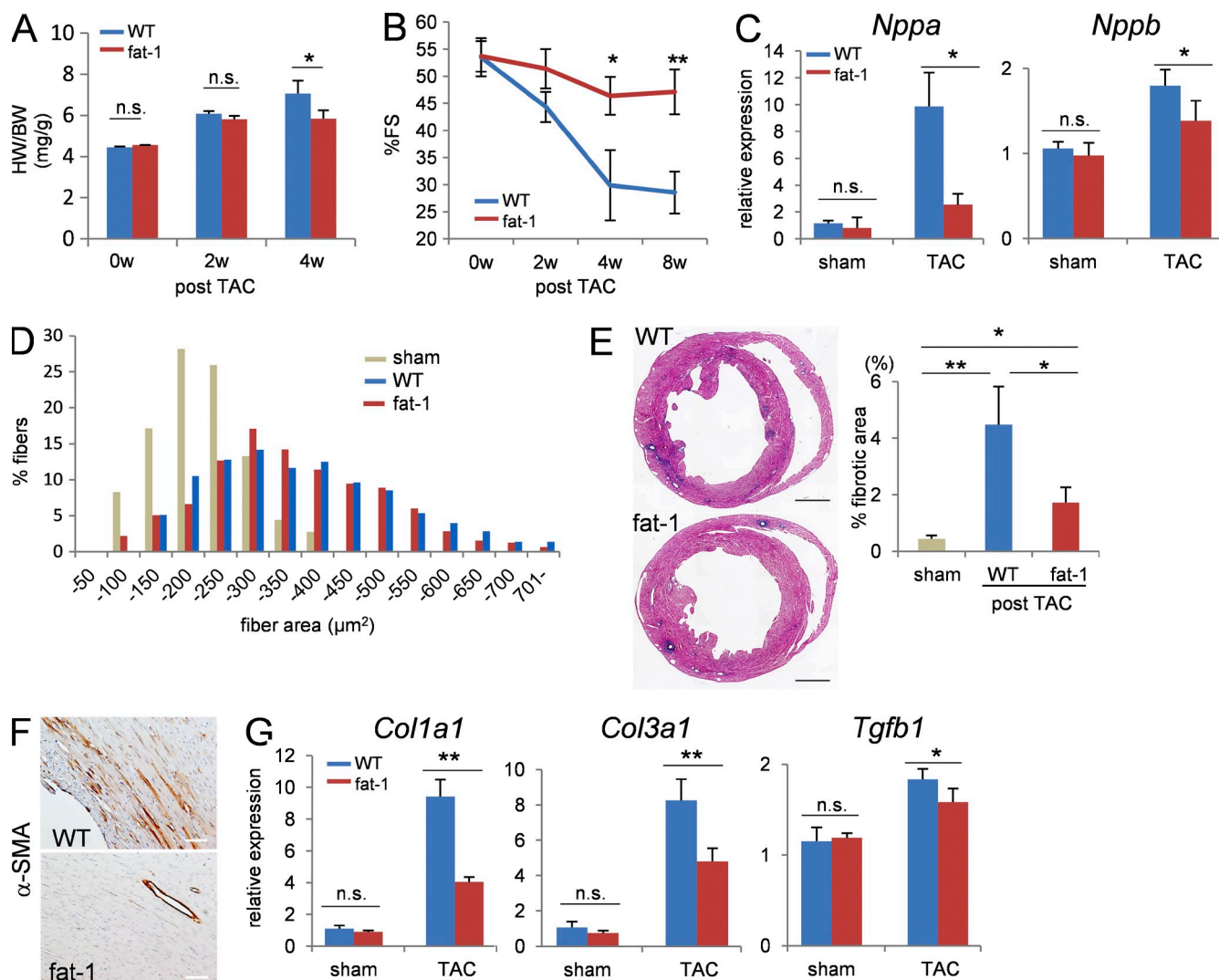
Figure 1. Fat-1 mice showed preserved LV function and less cardiac fibrosis than WT mice after TAC. (A) Heart weight/body weight (HW/BW) ratios from WT and fat-1 transgenic hearts. $n = 10$. (B) %FS after TAC measured by echocardiography. $n = 20$. (C) Relative expression levels of *Nppa* and *Nppb* mRNA 4 wk after TAC. Expression levels were normalized to those of 18s ribosomal RNA and then normalized with respect to those in the WT sham-operated hearts. $n = 10$. (D) Myocardial cross-sectional area (CSA) measured by staining with WGA at the papillary muscle level in ventricle section 4 wk after TAC. $n = 450–500$. (E, left) Representative low-magnification views of Azan staining of the heart sections 4 wk after TAC. Image is a compilation of two independent experiments. Bar, 1 mm. (right) Measurement of the fibrotic area in a ventricle section. *, $P < 0.05$; **, $P < 0.01$. Data in E were analyzed by Kruskal-Wallis tests followed by Bonferroni post-hoc analysis. (F) Myofibroblast transformation evaluated in heart sections stained with anti–α-SMA antibody. Bars, 100 μm. (G) Relative expression levels of cardiac fibrosis-associated genes (*Col1a1*, *Col3a1*, and *Tgfb1*). n.s. indicates not significant; *, $P < 0.05$; **, $P < 0.01$. Data in A–C and G were analyzed by Mann-Whitney U tests. Experiments were repeated three times and the data were pooled.

GFP$^+$ cells were significantly fewer in number in the fat-1/GFP → WT mice compared with WT/GFP → WT mice (Fig. 3 E). Notably, the majority of GFP$^+$ cells in the 4-wk post-TAC hearts were CD68$^+$ macrophages (Fig. 3 F).

Fat-1 transgenic BM cells contained markedly higher proportions of EPA compared with WT BM cells

We measured the n-6 and n-3 PUFA compositions in heart cells and BM cells from the chimeras by GC-MS (Fig. 3 G) and found that fatty acid composition differed among different cell types. The proportion of n-3 PUFAs (EPA [C20:5, n-3], DPA [C22:5, n-3], DHA [C22:6, n-3]) per total lipid was extremely low in BM cells (∼1% of total lipid), whereas the proportion of DHA per total lipid was markedly high in heart cells. The proportion of DHA was increased in the fat-1 transgenic heart cells (∼25% of total lipid) compared with WT heart cells (∼10% of total lipid), whereas the proportion of arachidonic acid (AA) was reduced in the fat-1 transgenic heart cells (∼7.5% of total lipid) compared with WT heart cells (∼15% of total lipid). Fatty acid composition was comparable
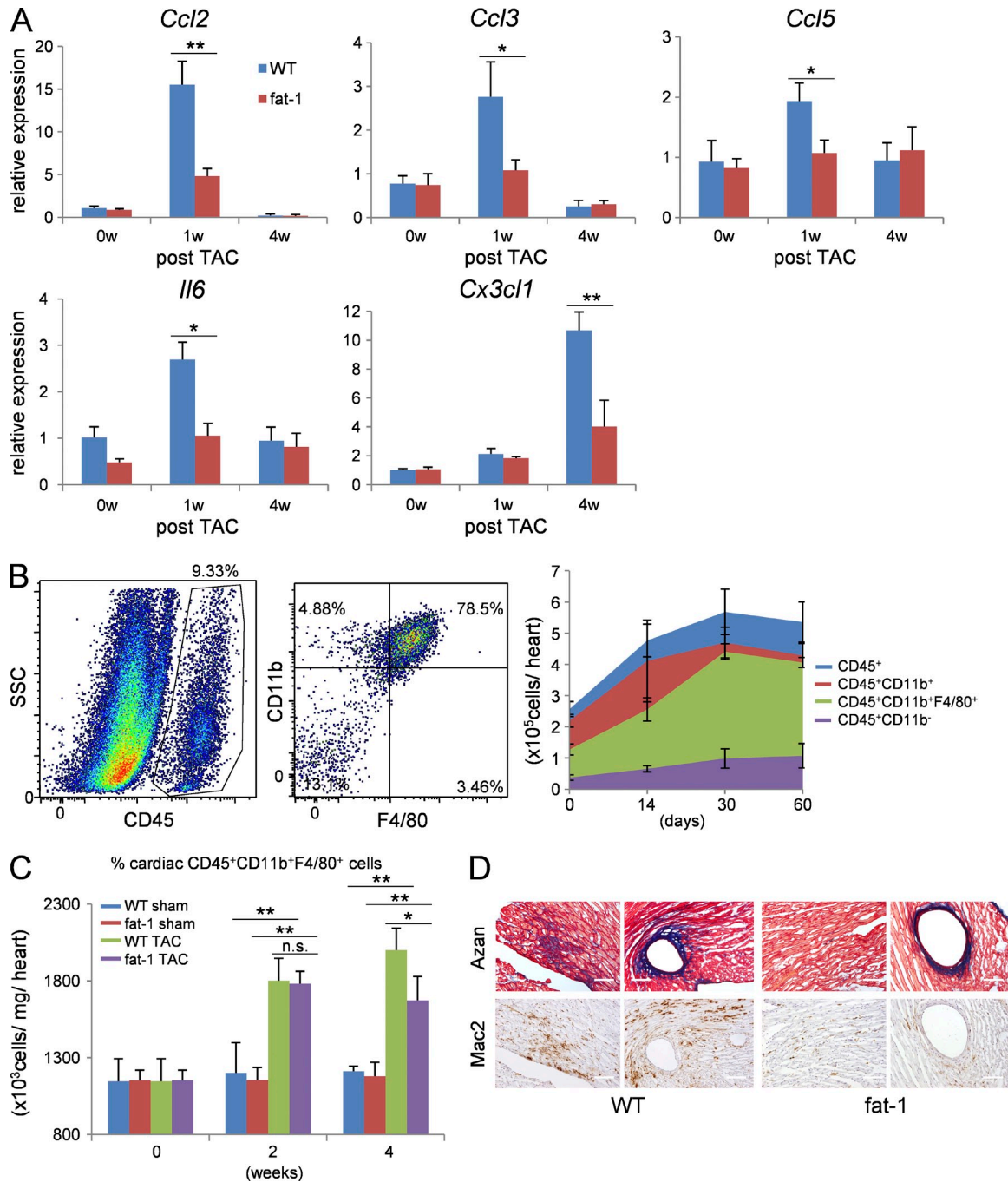
Figure 2. Fat–1 mice showed less macrophage infiltration in the heart after TAC than WT mice. (A) Relative expression levels of *Ccl2*, *Ccl3*, *Ccl5*, *Il6*, and *Cx3cl1* mRNA in WT and fat-1 transgenic hearts 0, 1, and 4 wk after TAC. *n* = 5. *, P < 0.05; **, P < 0.01. Data were analyzed by Mann-Whitney *U* tests. (B) FACS analysis of myocardial inflammatory cells. Macrophages were identified as CD45+, CD11b+, or F4/80+, as shown in the dot images (left). The temporal change in number of inflammatory cells in TAC hearts (right). *n* = 8. (C) Concentration of CD45+ CD11b+ F4/80+ cells per heart weight in WT and fat-1 transgenic hearts 0, 2, and 4 wk after TAC measured by flow cytometry. *n* = 8. n.s. indicates not significant; *, P < 0.05; **, P < 0.01. Statistical analysis was performed using Kruskal-Wallis tests followed by Bonferroni post-hoc analysis. (D) Activated macrophages expressing Mac2 accumulated in the fibrotic tissue area. Azan staining (top) and immunohistochemistry for Mac2 (bottom) in ventricle sections from WT or fat-1 mice 4 wk after TAC. Bars, 100 µm. Experiments were repeated three times and the data pooled.

between the fat–1 transgenic BM cells and WT BM cells except for EPA, which was increased markedly in the fat-1 transgenic BM cells (∼0.5% of total lipid) compared with WT BM cells (∼0.1% of total lipid).

Fat–1 transgenic macrophages were less potent in activating cardiac fibroblasts than WT macrophages

Next, we examined the distinct functions between WT macrophages and fat-1 transgenic macrophages in cardiac fibroblast
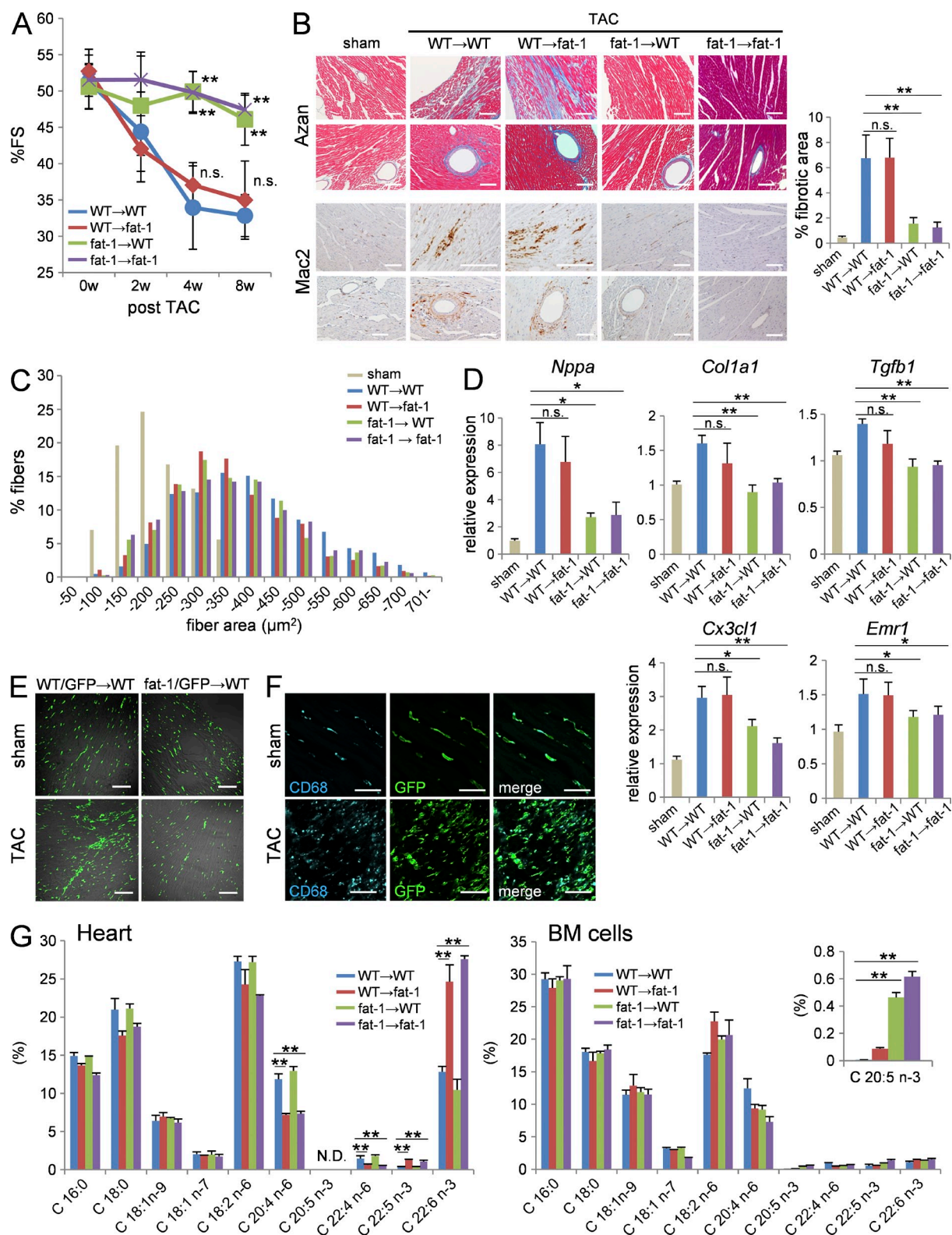
Figure 3. BM–derived cells elicited cardiac protection against pressure overload in fat–1 mice. (A) %FS of the prepared BMT chimeras subjected to TAC. *n* = 20. (B) Azan staining and immunohistochemistry for Mac2 in ventricle sections from the BMT chimera mice after TAC. Bars, 100 µm. (C) Myocardial CSA in ventricle section of BMT chimera mice subjected to pressure overload for 4 wk. *n* = 5; *n* = 450–500. (D) Relative expression levels of *Nppa*, *Col1a1*, *Tgfb1*, *Cx3cl1*, and *Emr1* in the hearts of BMT chimera mice 4 wk after TAC. Expression levels were normalized to those of 18S ribosomal RNA and then normalized with respect to those in the sham operated hearts. *n* = 6. (E) Immunofluorescence images for BM-derived GFP+ macrophages in ventricle
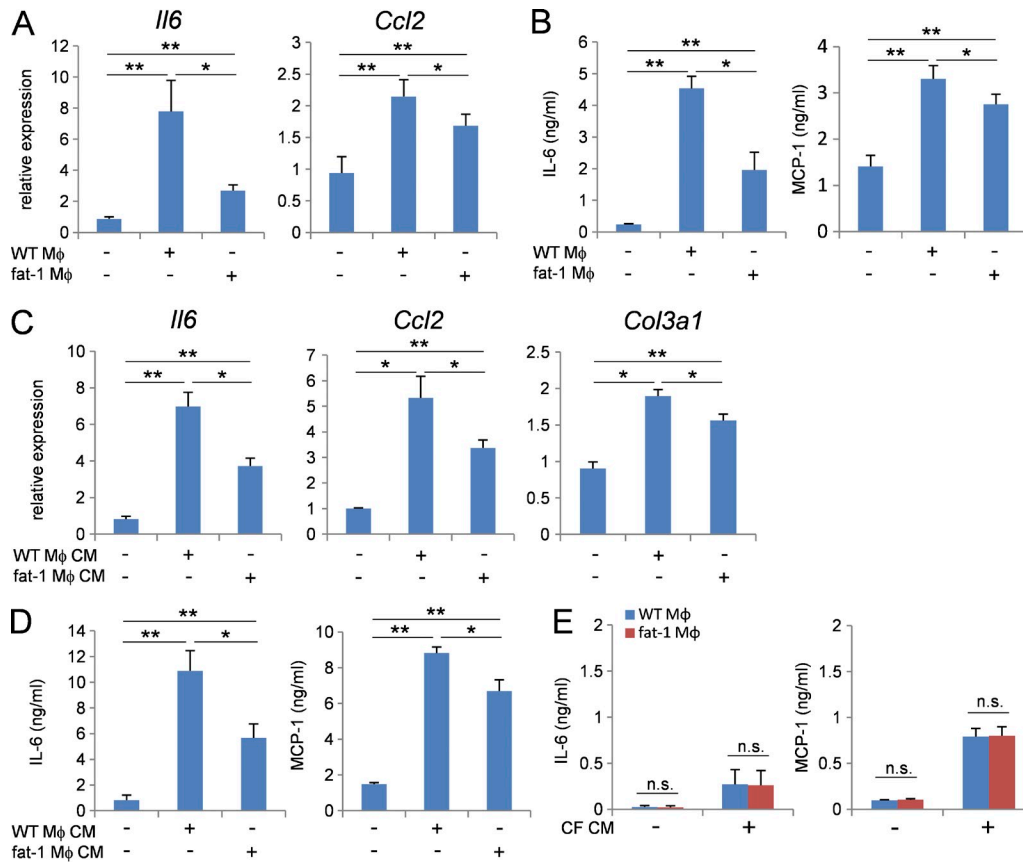
Figure 4. Fat-1 transgenic macrophages exerted anti-inflammatory effects when co-cultured with cardiac fibroblasts. (A) Relative expression levels of *Il6* and *Ccl2* mRNA in cardiac fibroblasts cultured with WT or fat-1 transgenic macrophages using a Transwell system for 48 h. n = 5. Expression levels were normalized to those of 18S ribosomal RNA and then normalized with respect to those in the vehicle sample. (B) Concentrations of IL-6 and MCP-1 in the culture medium of cardiac fibroblasts cultured with WT or fat-1 transgenic macrophages using a Transwell system and ELISA. n = 5. (C) Relative expression levels of *Il6*, *Ccl2*, and *col3a1* mRNA in cardiac fibroblasts stimulated with WT or fat-1 transgenic macrophage-conditioned medium for 48 h. n = 5. (D) Concentrations of IL-6 and MCP-1 in the culture medium of cardiac fibroblasts stimulated with WT or fat-1 transgenic macrophage-conditioned medium for 48 h. n = 5. (E) Concentrations of IL-6 and MCP-1 in the medium of WT or fat-1 transgenic macrophages stimulated with WT cardiac fibroblast-conditioned medium. n.s. indicates not significant; *, P < 0.05; **, P < 0.01. Statistical analysis was performed using Kruskal-Wallis tests followed by Bonferroni post-hoc analysis. Experiments were repeated twice.

activation. Co-culturing cardiac fibroblasts with WT macrophages in a Transwell culture chamber system increased the expressions of *Il6* and *Ccl2* mRNAs, but this effect was significantly less potent when co-culturing cardiac fibroblasts with fat-1 transgenic macrophages (Fig. 4 A). Consistent with this, co-culturing cardiac fibroblasts with WT macrophages increased the IL-6 and MCP-1 protein concentrations in culture media, but this effect was significantly less potent when co-culturing cardiac fibroblasts with fat-1 transgenic macrophages (Fig. 4 B). Similarly, stimulation of cardiac fibroblasts with WT macrophage-conditioned media up-regulated the expression of *Il6*, *Ccl2,* and *Col3a1*

mRNAs (Fig. 4 C) and resultant IL-6 and MCP-1 proteins (Fig. 4 D), whereas fat-1 transgenic macrophage–conditioned media had a less potent effect. In contrast, cardiac fibroblast–conditioned media equally stimulated both WT macrophages and fat-1 transgenic macrophages to produce IL-6 and MCP-1, although the levels produced were 40- and 10-fold less, respectively, than those produced by cardiac fibroblasts (Fig. 4 E). These in vitro studies indicated that fat-1 transgenic macrophages are less potent proinflammatory activators of cardiac fibroblasts, probably due to either reduced secretion of proinflammatory molecules or increased secretion of antiinflammatory molecules.

sections of sham- or TAC-operated heart from the chimeras transplanted with WT or fat-1/GFP double-transgenic BM. Bars, 100 µm. (F) The majority of GFP-positive cells in the sham or TAC-operated hearts from WT mice transplanted with the GFP transgenic BM expressed CD68, a macrophage marker (cyan). Bars, 50 µm. (G) The fatty acid composition of hearts and BM cells from the four BMT chimeras. n = 5. N.D. indicates not detected. n.s. indicates not significant; *, P < 0.05; **, P < 0.01 versus WT → WT BMT chimera group. Statistical analysis was performed using Kruskal-Wallis tests followed by Bonferroni post-hoc analysis. Experiments were repeated three times and the data pooled.
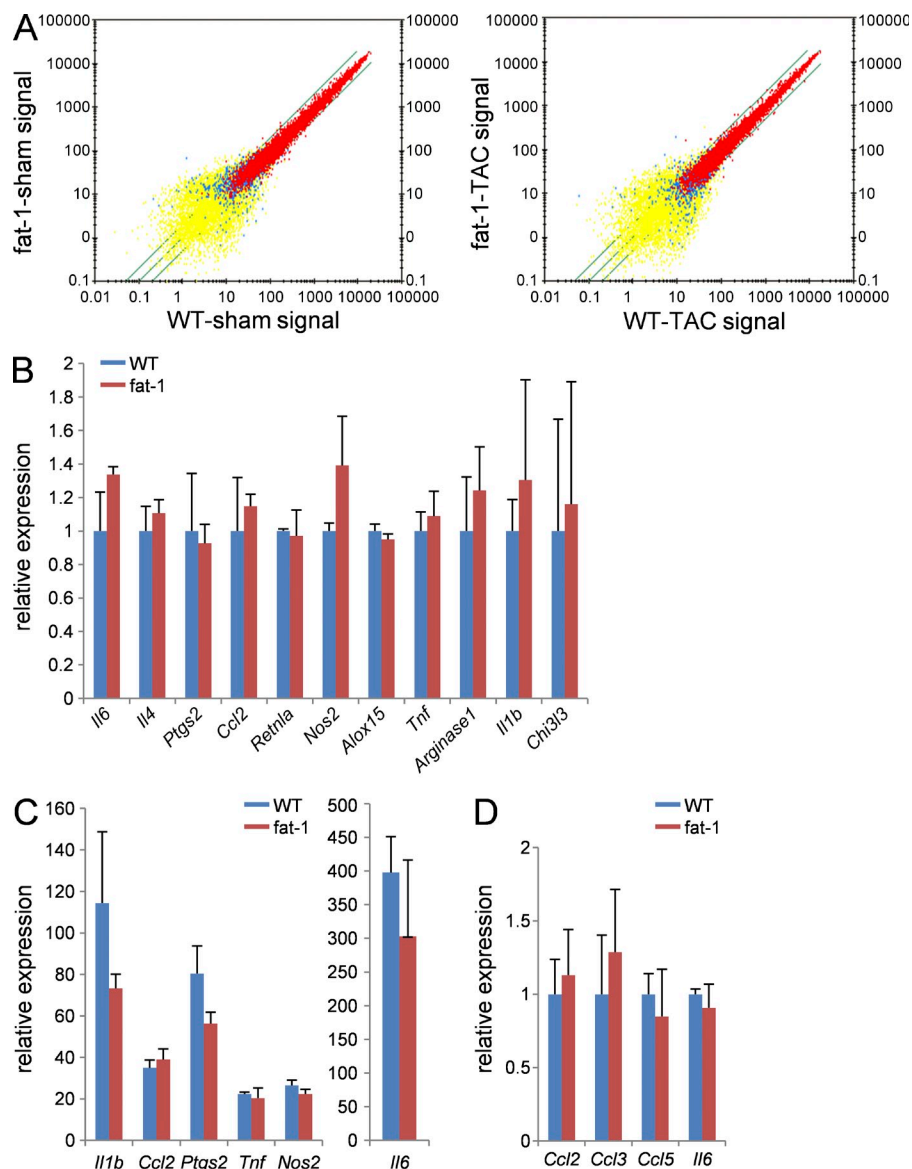
Figure 5. The gene expression profiles of macrophages were comparable between WT and fat-1 mice. (A) Dot plot comparisons of gene expression profiles among macrophages isolated from sham or 2 wk after TAC hearts of WT or fat-1 mice. (B and C) The relative gene expression levels of (B) resident peritoneal macrophages or (C) LPS-stimulated (1 µg/ml for 4 h) peritoneal macrophages from WT or fat-1 mice. $n = 5$. (D) The relative gene expression levels of blood monocytes (CD11b$^+$ Ly6C$^+$ Ly6G$^-$) from WT and fat-1 mice 3 d after TAC operation. $n = 4$. Expression levels were normalized to those of 18S ribosomal RNA and then normalized with respect to those in (B and C) WT resident peritoneal macrophage or (D) WT circulating monocytes. Data were analyzed by (B and D) Mann-Whitney U tests or (C) Kruskal-Wallis tests followed by Bonferroni post-hoc analysis. Experiments were repeated twice and the data were pooled.

An EPA-derived metabolite, 18-HEPE, suppressed cardiac fibroblast activation

To examine the impact of EPA enrichment on gene expression in macrophages, we compared the gene expression profiles between WT and fat-1 transgenic macrophages. The expression of inflammation-related genes in macrophages isolated from post-TAC hearts was comparable between WT and fat-1 mice (Fig. 5 A), as was the expression of M1 or M2 marker genes (Fig. 5, B and C). Also, there was no difference in the expression levels of inflammatory genes (Ccl2, Ccl3, Ccl5, and Il6) in circulating monocytes between WT and fat-1 mice under pressure overload (Fig. 5 D). Therefore, we speculated that free fatty acid and the resulting metabolites released among macrophages are responsible for the distinct phenotypes observed in WT mice and fat-1 mice under the pressure-overload conditions.

To confirm this hypothesis, lipids were extracted from both WT macrophage and fat-1 transgenic macrophage-conditioned media. Cardiac fibroblasts were stimulated with WT macrophage-conditioned media either in the presence or absence of lipid extracts (Fig. 6 A). Notably, the lipid extracts from WT macrophage-conditioned media did not further increase IL-6 production by cardiac fibroblasts, whereas the lipid extracts from fat-1 transgenic macrophage-conditioned media significantly suppressed IL-6 production by cardiac fibroblasts.

Next, we performed LC-MS/MS-based lipidomic analysis of AA and EPA metabolites released into the WT macrophage- and fat-1 transgenic macrophage-conditioned media (Fig. 6 B). Among EPA metabolites, the levels of 12-HEPE, 15-HEPE, and 18-HEPE were higher in fat-1 transgenic macrophage-conditioned media than in WT macrophage-conditioned media. Among AA metabolites, the levels of TXB2 and PGE2 were increased, whereas 12-HETE was decreased in fat-1 transgenic macrophage-conditioned media compared with WT macrophage-conditioned media. Then, we stimulated cardiac
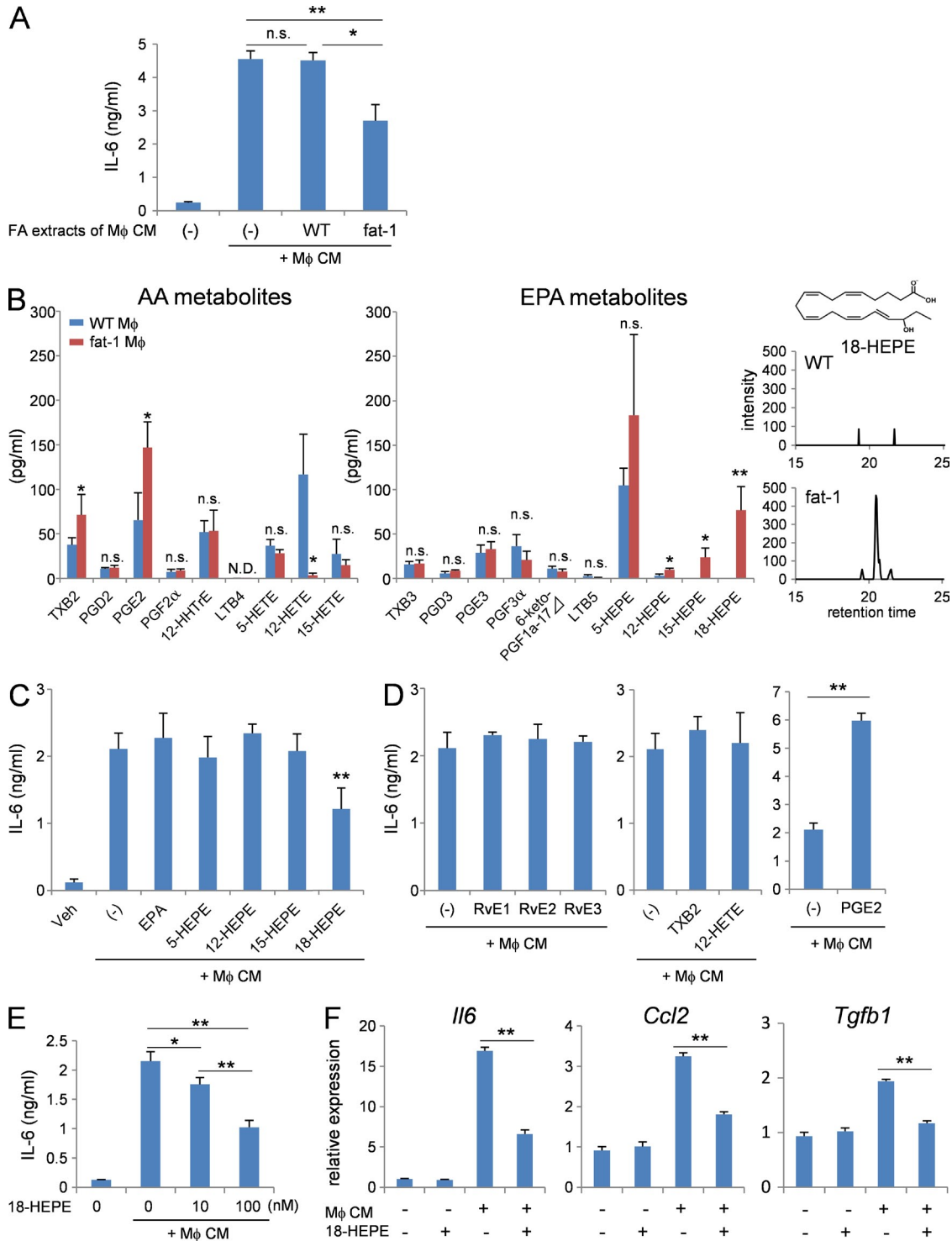
Figure 6.   Mediator lipidomics identified 18–HEPE as a major EPA metabolite released by fat-1 transgenic macrophages. (A) Concentration of IL-6 in culture medium of the cardiac fibroblasts stimulated with macrophage-conditioned medium in the presence of fatty acid extracts from WT or fat-1 transgenic macrophage-conditioned medium. $n = 5$. (B) LC-MS/MS-based lipidomic analysis of WT or fat-1 transgenic macrophage-conditioned medium. 18-HEPE was monitored by MRM mode using the established transition (317 > 259 m/z). $n = 4$. *, $P < 0.05$; **, $P < 0.01$. Data in B were analyzed by Mann-Whitney U tests. (C–E) Concentrations of IL-6 in the culture medium of cardiac fibroblasts stimulated with macrophage-conditioned medium in the presence of (C) 100 nM EPA, 5-, 12-, 15-, 18-HEPE; (D) RvE1, RvE2, RvE3, TXB2, 12-HETE, and PGE2; or (E) 10 and 100 nM 18-HEPE. $n = 5$. (F) Relative expression levels of *Il6*, *Ccl2*, and *Tgfb1* mRNA of cardiac fibroblasts stimulated with macrophage-conditioned medium in the presence of 100 nM 18-HEPE. $n = 5$. N.D. indicates not detected. n.s. indicates not significant; *, $P < 0.05$; **, $P < 0.01$. Data in A and C–F were analyzed by Kruskal-Wallis tests followed by Bonferroni post-hoc analysis. Experiments were repeated twice.

fibroblasts with WT macrophage-conditioned media either in the presence or absence of 100 nM EPA, 5-HEPE, 12-HEPE, or 18-HEPE (Fig. 6 C). Among them, only 18-HEPE suppressed IL-6 production from cardiac fibroblasts. Metabolites of 18-HEPE, namely RvE1, E2, and E3 had no effect on IL-6 production from cardiac fibroblasts. Among metabolites of AA, TXB2 and 12-HETE had no effect on IL-6 production from cardiac fibroblasts, whereas 100 nM PGE2 increased production (Fig. 6 D). We observed dose-dependent suppression of IL-6 production from cardiac fibroblasts exposed to 18-HEPE, with 10 nM a sufficient concentration to elicit this effect (Fig. 6 E). The increased expression of *Il-6*, *Ccl2*, and *Tgfb1* mRNA in cardiac fibroblasts with WT macrophage-conditioned media was also significantly attenuated by 18-HEPE (Fig. 6 F).

BM-derived cells generated an 18-HEPE–rich milieu in fat-1 transgenic heart
LC-MS/MS-based lipidomic analyses of lipid mediators revealed that the levels of EPA and its monooxygenated product 18-HEPE were selectively elevated in sham-operated fat-1 transgenic hearts compared with sham-operated WT hearts (Fig. 7, A and B), and these levels remained elevated in the fat-1 transgenic hearts at 4 wk after TAC. In contrast, AA and its metabolites in sham-operated hearts were comparable between WT and fat-1 transgenic mice. The levels of AA metabolites PGE2 and 12-HETE, prostanoids known to be involved in cardiac fibrosis and inflammation, were comparable between WT and fat-1 transgenic mice at 4 wk after TAC.

Finally, the BMT study revealed that levels of both EPA and 18-HEPE were appreciably high in the hearts of fat-1 → WT and fat-1 → fat-1 chimera compared with WT → WT and WT → fat-1 chimera (Fig. 6 C). These findings indicated that 18-HEPE in fat-1 transgenic hearts were mostly derived from BM cells.

Plasma 18-HEPE concentrations increased after oral administration of EPA in humans
We next asked whether dietary intake of EPA could increase plasma levels of 18-HEPE in humans. LC-MS/MS was used to measures a series of fatty acid metabolites in fasting plasma from healthy volunteers who took oral doses of high-purity EPA ethyl ester (2,700 mg/day Epadel) for 14 d (Table 1). Dietary intake of EPA significantly increased the plasma concentration of 18-HEPE compared with controls not fed with EPA (95.6 ± 23.7 pg/ml vs. 149.0 ± 12.7 pg/ml; P = 0.000721; Table 1). The plasma concentration of other EPA metabolites, including RvE2 and RvE3, were not significantly increased under this condition.

Administration of 18-HEPE prevented pressure overload–induced cardiac fibrosis and inflammation
Lastly, we examine the therapeutic effect of 18-HEPE on maladaptive cardiac remodeling under pressure overload. Previous studies demonstrated that administration of EPA, which

is usually given orally at 3–10 mg/day, prevented pressure overload–induced cardiac dysfunction (Duda et al., 2007; Chen et al., 2011).

Notably, 18-HEPE administered at a dose of 1 or 5 µg by intraperitoneal injection every 3 d from the beginning of pressure overload significantly mitigated the reduction in %FS (Fig. 8 A), as well as increases in perivascular and interstitial fibrosis (Fig. 8 B), macrophage infiltration (Fig. 8 C), and expression of *Nppa*, *Col1a1*, *Tgfb1*, *Cx3cl1*, and *Emr1* mRNA (Fig. 8 D), without affecting cardiomyocyte hypertrophy (Fig. 8 E) at 4 wk after TAC. The protective effect of 18-HEPE was compatible with the phenotype observed for fat-1 transgenic mice. Notably, the same dose of EPA had no effect on pressure overload–induced cardiac fibrosis and inflammation.

To clarify whether a delayed application of 18-HEPE can also exert a therapeutic effect on maladaptive cardiac remodeling under pressure overload, we started the 18-HEPE administration 1 wk after TAC surgery. A delayed application of 18-HEPE was similarly effective (Fig. 8, F and G).

DISCUSSION
Using fat-1 transgenic mice carrying *C. elegans* n-3 fatty acid desaturase, which is capable of producing n-3 PUFAs from n-6 PUFAs, we demonstrated the potential mechanisms by which n-3 PUFA exhibits resistance to pressure overload–induced cardiac remodeling. Sustained communication between cardiac fibroblasts and BM-derived immune cells, especially macrophages, play a key role in the progression of cardiac fibrosis. Activated cardiac fibroblasts produce proinflammatory cytokines and chemokines, such as IL-6 and MCP-1, facilitating macrophage activation (Koyanagi et al., 2000; Sano et al., 2000; Kuwahara et al., 2004; Kayama et al., 2009; Meléndez et al., 2010; Ma et al., 2012). Cardiac fibroblasts can be activated directly by pressure overload or secondarily by inflammatory mediators released from activated inflammatory cells (Nicoletti et al., 1996; Koyanagi et al., 2000; Kuwahara et al., 2004; Kai et al., 2006). This pro-fibrotic feed-forward loop accelerated the progression of cardiac fibrosis under pressure overload. We demonstrated here that BM-derived and EPA-enriched fat-1 transgenic macrophages generated an 18-HEPE-rich milieu in the heart, thereby counter-regulating the profibrotic feed-forward loop established under pressure-overload conditions.

BMT studies indicated the importance of BM cells in the observed protective effects against cardiac remodeling. Protection conferred by the fat-1 transgenic BM cells was comparable between fat-1 → WT and fat-1 → fat-1 chimeric mice in this study, indicating that the fat-1 transgenic BM cells accounted for the full effect of the fat-1 transgene on cardiac remodeling, and the contribution of cardiomyocytes to adaptive changes in fat-1 mice was minor, if any. Using lipidomic analysis, we identified selective enrichment of EPA in fat-1 transgenic BM cells and the EPA monooxygenated metabolite, 18-HEPE, in fat-1 transgenic macrophages. Furthermore, the levels of EPA and 18-HEPE were selectively increased in fat-1 transgenic hearts compared with sham-operated WT

hearts. The BMT study also demonstrated that both EPA and 18-HEPE levels in the hearts were appreciably high in fat-1 → WT and fat-1 → fat-1 chimera, whereas levels were very low in WT → WT and WT → fat-1 chimera. Collectively, these results indicated that 18-HEPE in fat-1 transgenic hearts mostly derived from BM cells.
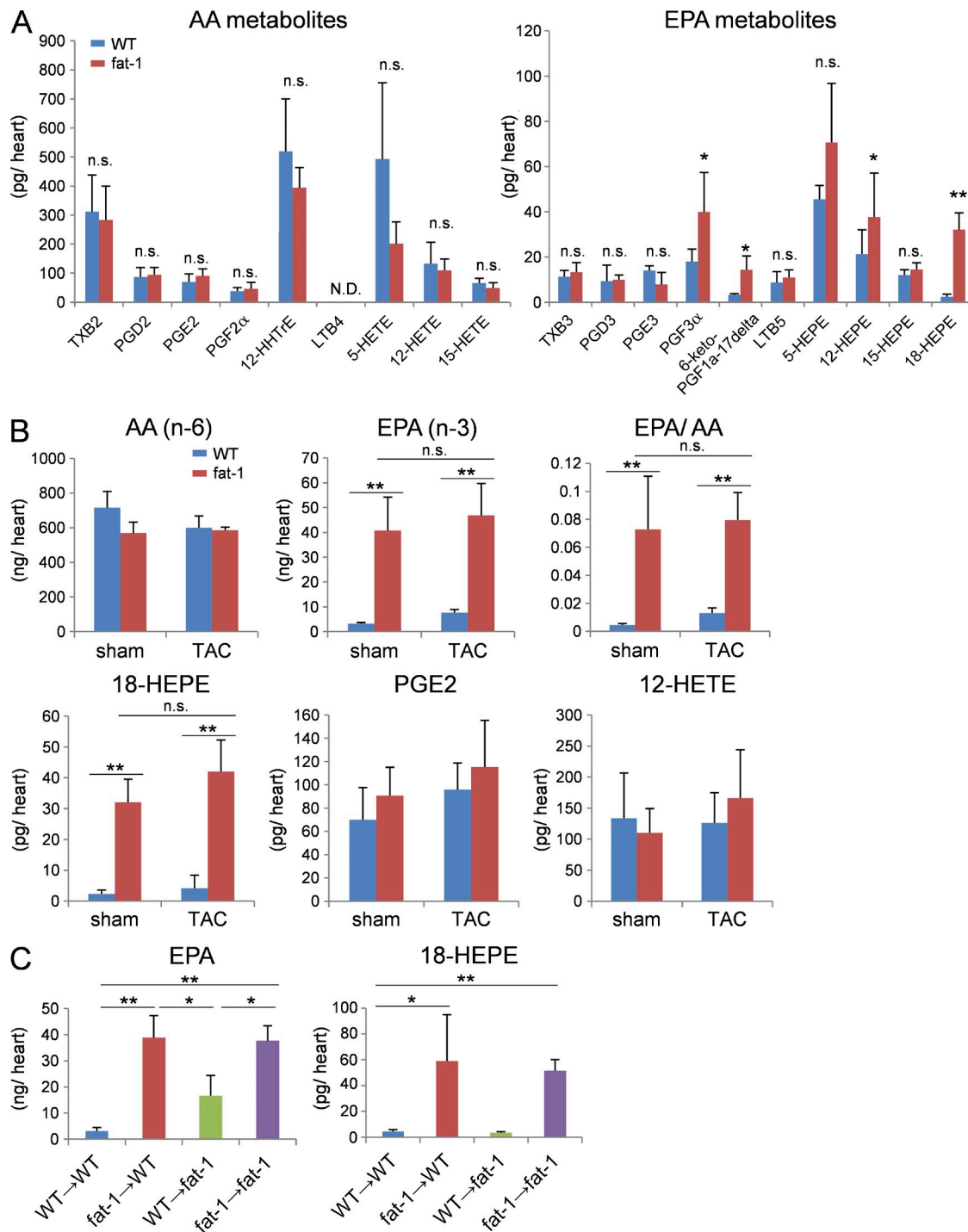

Figure 7.   **18–HEPE enriched in fat–1 transgenic heart was mainly produced by the BM–derived cells.** (A) LC-MS/MS-based lipidomic analysis of the hearts from WT or fat-1 mice. $n = 4$. Data were analyzed by Mann-Whitney U tests. (B) The level of AA, EPA, 18-HEPE, PGE2, and 12-HETE production of pre- or post-TAC hearts from WT or fat-1 mice measured by LC-MS/MS. $n = 4$. (C) The level of EPA and 18-HEPE production of hearts from the four BMT chimeras. $n = 4$. Data in (B and C) were analyzed by Kruskal-Wallis tests followed by Bonferroni post-hoc analysis. Experiments were repeated twice. N.D. indicates not detected. n.s. indicates not significant; *, $P < 0.05$; **, $P < 0.01$.

Table 1. Profile of lipid mediators in human plasma of healthy volunteers taking dietary EPA at 2.7 g/day

EPA–derived lipid mediator	EPA 0w (pg/ml)	EPA 2w (pg/ml)	P value
PGE_3	26.4 ± 5.9	32.0 ± 13.2	0.699428347
PGD_3	7.2 ± 2.7	9.9 ± 3.4	0.506270699
$PGF_{3\alpha}$	90.3 ± 33.8	80.5 ± 44.2	0.825358514
6-keto-PGF_{1a}-17delta	72.4 ± 48.4	80.6 ± 71.4	0.772022261
TXB_3	10.8 ± 3.6	16.6 ± 6.8	0.243550461
LTB_5	7.6 ± 1.6	10.9 ± 1.5	0.301981898
LXA_5	3.2 ± 1.5	15.2 ± 5.7	0.526795284
RvE2	10.1 ± 4.1	24.9 ± 13.5	0.397489159
RvE3	55.3 ± 8.5	42.3 ± 13.8	0.349509121
5-HEPE	309.7 ± 84.2	270.1 ± 51.8	0.756489821
8-HEPE	48.7 ± 13.3	88.9 ± 25.7	0.060813559
9-HEPE	55.0 ± 18.1	95.3 ± 17.9	0.151960325
8,9-EpETE	29.6 ± 10.0	68.7 ± 37.7	0.341822254
11-HEPE	36.3 ± 9.1	44.0 ± 8.9	0.471267817
12-HEPE	58.8 ± 17.5	72.2 ± 12.8	0.351678213
11,12-EpETE	109.9 ± 27.2	257.5 ± 138.6	0.335749115
15-HEPE	149.3 ± 24.4	188.2 ± 36.0	0.346843422
14,15-EpETE	46.8 ± 14.6	131.5 ± 86.8	0.416135401
18-HEPE	95.6 ± 23.7	149.0 ± 12.7	0.000720547
17,18-EpETE	144.8 ± 46.3	220.3 ± 98.1	0.463858736
17,18-diHETE	3855.4 ± 371.3	7364.9 ± 928.5	0.002201551
19-HEPE	584.5 ± 126.9	1205.3 ± 195.8	0.038534813
20-HEPE	189.3 ± 62.5	266.4 ± 30.3	0.153533361
5,15-diHEPE	9.9 ± 3.4	20.2 ± 7.3	0.372063162
8,15-diHEPE	37.7 ± 5.6	32.7 ± 9.5	0.618181239
8,18-diHEPE	6.8 ± 3.3	15.3 ± 4.9	0.068913138
12,18-diHEPE	11.1 ± 4.9	24.7 ± 5.6	0.068628042

Flow cytometric analysis in this study identified macrophages as the major type of leukocytes in all heart tissues. It also showed that macrophage numbers in heart gradually increased after TAC and remained elevated for at least 60 d. Consistent with this, BMT studies using WT/GFP transgenic mice and fat-1/GFP double-transgenic BM revealed equal numbers of BM-derived GFP^+ cells in the hearts of WT/GFP →WT and fat-1/GFP →WT mice before TAC surgery, and an increased number under pressure overload. Notably, the majority of GFP^+ cells in the hearts were $CD68^+$ macrophages. Together, these results indicated that the 18-HEPE–rich milieu in the fat-1 transgenic heart was generated by BM-derived macrophages.

Blood monocytes are recruited to heart in the early phase of left ventricular pressure overload. $Ly-6C^{high}$ monocytes selectively express CCR2, a receptor for MCP-1, whereas $Ly-6C^{low}$ monocytes express high levels of CX3CR1, a receptor for Fractalkine (Nahrendorf et al., 2007; Epelman et al., 2014). We also found herein that pressure-overloaded hearts modulate their chemokine expression profile over time. *Ccl2* (MCP-1) mRNA levels peaked at 1 wk after TAC, whereas *Cx3cl1* (Fractalkine) mRNA levels peaked at 4 wk after TAC. These findings suggested a biphasic response of monocytes to myocardial mechanical injury. Because both *Ccl2* (MCP-1)

mRNA levels and *Cx3cl1* (Fractalkine) mRNA levels were suppressed in fat-1 transgenic hearts, we speculate that the sequential recruitment of monocyte subsets was attenuated in fat-1 transgenic hearts. However, it remains unknown what proportion of monocytes differentiated into macrophages after being recruited to the pressure-overloaded hearts, although reported turnover rates of monocytes in injured heart are <24 h (Leuschner et al., 2012). Our experimental results indicated that the majority of 18-HEPE was generated by preexisting macrophages and hence focused on the communication between cardiac fibroblasts and macrophages in terms of the profibrotic feed-forward loop accelerating the progression of cardiac fibrosis under pressure overload in this study. Future studies are necessary to elucidate the relative contribution of other fat-1 transgenic immune cells to cardiac fibrosis under pressure overload, including different monocyte subsets.

We stimulated cardiac fibroblasts with WT macrophage-conditioned media either in the presence or absence of 100 nM of EPA, 18-HEPE, RvE1, RvE2, and RvE3. Among them, only 18-HEPE blunted IL-6 production from cardiac fibroblasts, whereas RvE1, RvE2, and RvE3 at the same concentration had no such effect. In humans, dietary intake of high-purity EPA ethyl ester (2,700 mg/day Epadel) significantly increased the plasma concentration of 18-HEPE compared with controls

not fed with EPA (95.6 ± 23.7 pg/ml vs. 149.0 ± 12.7 pg/ml; P = 0.000721). The plasma concentrations of other EPA metabolites including RvE2 and RvE3 were not significantly increased after oral administration of EPA. In mice, previous studies demonstrated that EPA alleviates pressure overload–induced cardiac dysfunction when given orally at 3–10 mg/day
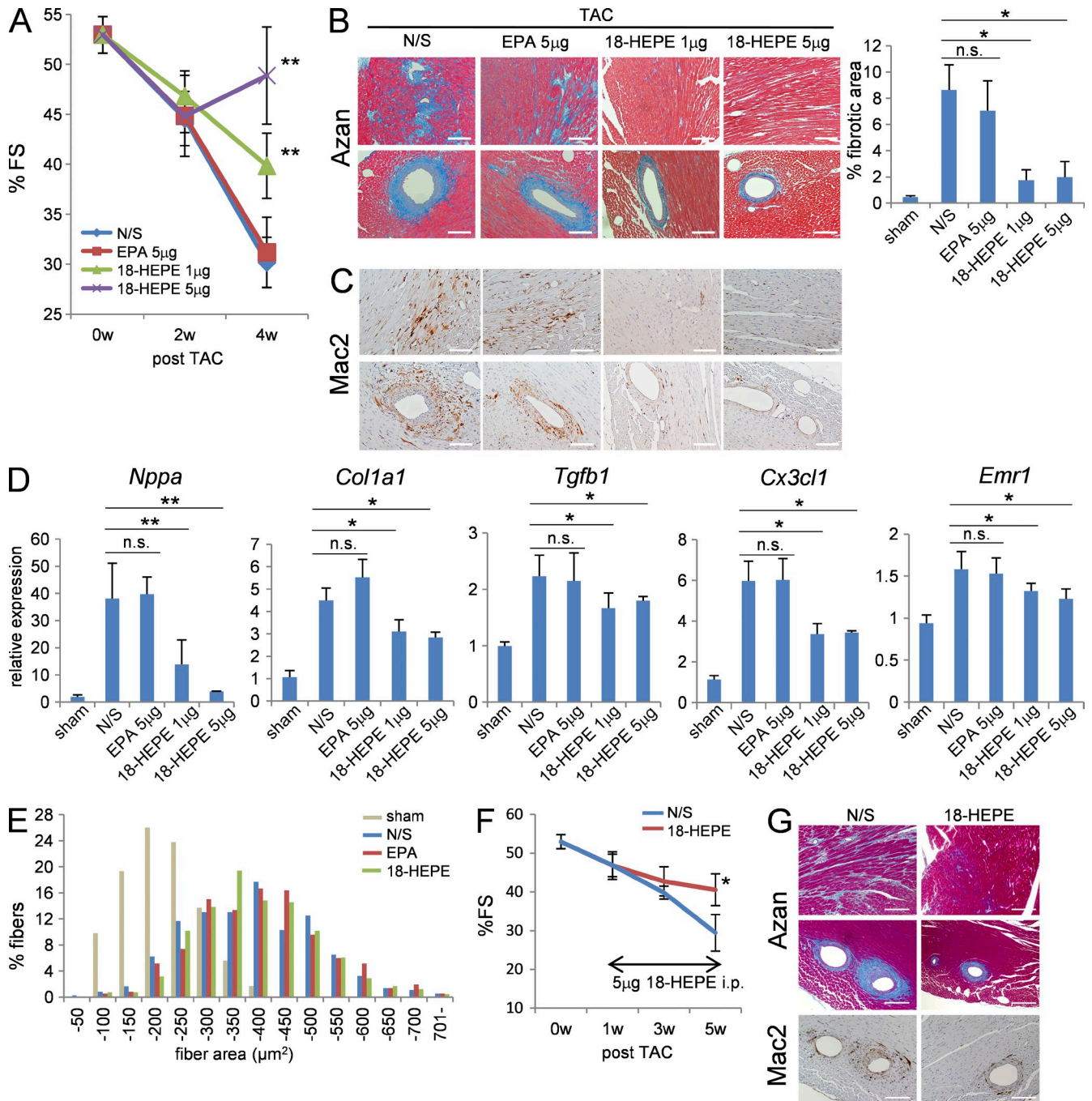

Figure 8. **18–HEPE administration elicited cardioprotection in TAC–operated mice.** (A) %FS of post-TAC mice administered with NS, 5 μg EPA, 1 μg or 5 μg 18-HEPE i.p. every 3 d. n = 12–20. (B) Azan staining and (C) immunohistochemistry for Mac2 in ventricle sections of the mice administered with 18-HEPE after TAC. Bars, 100 μm. (D) Relative expression levels of *Nppa*, *Col1a1*, *Tgfb1*, and *Emr1* mRNA in hearts from mice administered with 18-HEPE 4 wk after TAC. Expression levels were normalized to those of 18S ribosomal RNA, and then normalized with respect to those in the sham-operated hearts. n = 7. (E) Myocardial CSA in ventricle section of pressure-overloaded heart from the mice administered with NS, 5 μg EPA or 5 μg 18-HEPE. n = 5; n = 450–500. (F and G) 18-HEPE administration at 1 wk after TAC induction could prevent cardiac remodeling. (F) %FS of the mice administered with 18-HEPE at 5 μg every 2 d from 1 wk after TAC. n = 16. (G) Azan staining and immunohistochemistry for Mac2 in ventricle sections from the mice administered with 18-HEPE from 1 wk after TAC induction. Bars, 100 μm. n.s. indicates not significant; *, P < 0.05; **, P < 0.01 vs. N/S control group. Data in A, B, D, and F were analyzed by Kruskal-Wallis tests followed by Bonferroni post-hoc analysis. Experiments were repeated three times and the data pooled.

(Duda et al., 2007; Chen et al., 2011). In this study, 18-HEPE administered at a dose of 5 µg by intraperitoneal injection every 3 d was sufficient to achieve the same effect and plasma 18-HEPE concentrations reached ~30 pg/ml at 3 h after injection. In culture, n-3 fatty acids at 100 µM reportedly stimulate GPR120 production and mediate anti-inflammatory effects (Oh et al., 2010), whereas again here, we demonstrated a maximal such effect with 18-HEPE at 10 nM. Therefore, we strongly speculate that the physiological function of 18-HEPE is mediated through the high-affinity receptor.

Further work is needed to clarify the relationship between the fatty acid metabolome and cardiac pathology, with the ultimate goal to develop a novel therapeutic application for heart failure based on antiinflammatory and antifibrotic lipid mediators.

MATERIALS AND METHODS

Animals. Fat-1 mice (C57BL/6 background) were bred in the University of Tokyo animal facility. Fat-1 mice and the WT littermates were fed a special diet (AIN-76A; Oriental Yeast Co., Ltd) containing 9.4% safflower oil with a fatty acid composition of C18:1 n-9 (8–25%) and C18:2 n-6 (60–80%). WT littermates were always used as controls for the experiments involving fat-1 mice. In the 18-HEPE administration study, WT C57BL/6 mice were purchased at 5 wk of age from CLEA Japan Inc. and then fed the safflower oil–containing special diet described above. After 2 wk passed, the mice were subjected to TAC operation and then subsequently fed the same special diet. The University of Tokyo Animal Committee approved all experimental procedures and protocols.

Blood collection. This study evaluated peripheral blood from healthy human volunteers who took high-purity EPA ethyl ester 2.7 g/day for 14 d (protocol 20130089, approved by the Ethics Committee of Keio University, Tokyo, Japan; written informed consent was obtained from all donors). Fasting venous blood (5 ml) was collected from each donor before and 2 wk after EPA administration. Plasma was separated by centrifugation, and then added to 2 ml methanol. Samples were stored at −20°C for 2 h to precipitate plasma proteins and preserved at −80°C until extraction. Upon extraction, precipitated plasma proteins were separated by centrifugation and the supernatant was used for extraction.

Materials. EPA, 18-HEPE, RvE1, and other fatty acid metabolites were obtained from Cayman Chemical. RvE2 and RvE3 were chemically synthesized as described previously (Ogawa et al., 2009; Isobe et al., 2013).

BM transplantation. BM cells were harvested from the femurs and tibias of 8-wk-old recipient mice. After irradiation with a lethal dose of 10 Gy, the unfractionated BM cells (10^6 cells) were transferred intravenously into the irradiated donor mice, which were then allowed to rest for 8 wk. Success of the BMT was confirmed by positive detection of the fat-1 transgene in peripheral blood cells from the recipient mice using PCR, and then flow cytometry to assess the frequency of GFP-positive cells among peripheral nucleated blood cells from the transgenic mice was used to determine chimeric rates after BMT.

Generation of LV hypertrophy by transverse aortic constriction. Mice were subjected to LV pressure overload by TAC as previously described (Endo et al., 2007). In brief, mice were ventilated with 2% isoflurane in room air. The chest cavity was then exposed by cutting open the second left intercostal space. After isolating the aortic arch between the innominate and left common carotid arteries, it was constricted with a 7–0 nylon suture tied firmly three times against a 27-gauge blunted needle. Control mice were subjected to sham operations, and all animals were studied at 2, 4, and 8 wk after surgery.

Echocardiography and hemodynamic measurements. Mice were anesthetized by 1.5% isoflurane inhalation, and then anchored to a positioning platform in the supine position. Short-axis echocardiographic and Doppler echocardiographic measurements were made using the Vevo 660 system (Visual Sonics) with a 600 series real-time microvisualization scanhead probe. The LV internal end-systolic and end-diastolic diameters (LVESD and LVEDD, respectively) were measured using the leading-edge convention adopted by the American Society of Echocardiography. LV fractional shortening (FS) was calculated according to the formula: FS (%) = ([LVEDD − LVESD]/LVEDD) × 100. Heart rate did not differ significantly among the groups during the echocardiographic assessments.

Histological analysis and immunostaining. Mice were anesthetized and sacrificed. Hearts were then immediately perfused with PBS, fixed with 10% formalin neutral buffer solution, and embedded in paraffin. After deparaffinization, the sections were incubated in 0.3% H_2O_2 for 15 min and blocked in 5% BSA for 30 min at room temperature. Next, the sections were incubated with anti–Mac-2 antibody (clone M3/38; eBioscience; 1:200) or anti–α-smooth muscle actin antibody (α-SMA, clone 1A4; Sigma-Aldrich; 1:200) overnight at 4°C. Secondary antibodies conjugated with HRP were applied for 1 h at 4°C. Antibody binding was detected by incubating the sections in DAB substrate for 10 min at room temperature.

To evaluate the fibrotic area, short-axis sections at the mid LV level were stained with Azan and analyzed quantitatively against control reference sections using BZ-II Analyzer software (Keyence) on a BIOREVO BZ-9000 microscope (Keyence). The number of pixels with the predetermined level of blue tone were counted in each section, and then automatically converted into dimensions.

For immunofluorescence staining, the sections were incubated with anti-CD68 antibody (clone FA-11; AbD Serotec) overnight at 4°C, and then in secondary antibodies conjugated with TRITC (Dako; 1:200) for 1 h at 4°C. Nuclei were stained with Topro (Molecular Probes) in mounting medium, and the slides were observed by confocal laser-scanning microscopy (LSM510; Carl Zeiss) using appropriate emission filters.

Isolation and culture of adult murine cardiac fibroblasts. Hearts were perfused and digested with collagenase II (Worthington Biochemical Corp). Dissociated cells were incubated with anti-CD45-conjugated microbeads (Miltenyi Biotec), followed by selective depletion of CD45+ cells using autoMACS (Miltenyi Biotec). The remaining CD45- cells were resuspended in DMEM (Life Technologies) containing 10% fetal bovine serum and placed on Primaria culture dishes (BD). After 2 h, the culture medium was changed to remove any myocytes and endothelial cells still weakly attached to the dish. After 24 h, the culture medium was changed again, and the fibroblast cultures were grown to 85% confluence, at which point the medium was replaced with DMEM containing 0.1% FBS (serum-reduced medium). After a further 24 h, the isolated fibroblasts were cultured with co-cultured macrophages and macrophage-conditioned medium with or without 18-HEPE (Cayman Chemical).

Co-culture of cardiac fibroblasts with macrophages. Macrophages were isolated from peritoneal lavage by using anti-CD11b microbeads (Miltenyi Biotec) on autoMACS (Miltenyi Biotec). Adult murine cardiac fibroblasts (5×10^5 cells/well) were co-cultured with CD11b$^+$ peritoneal macrophages (5×10^5 cells/well) on 24-well plates using Transwell inserts (Corning) with a 0.4-µm porous membrane or with conditioned medium harvested from the 24-h CD11b$^+$ macrophage cultures. After incubation for 48 h, the supernatants and the cultured cells on the lower dish were harvested, and ELISA was used to determine IL-6 concentrations in the supernatants, according to the manufacturer's instructions (R&D Systems).

RNA extraction and real-time PCR. Total RNA was extracted by acid guanidinium thiocyanate-phenol-chloroform extraction with ISOGEN reagent (Nippon Gene). Reverse transcription was performed using the Prime Script RT reagent kit (Takara) in accordance with the manufacturer's protocol. Real-time PCR was performed using the SYBR Premix Ex Taq kit (Takara)

in an ABI Prism 7500 sequence detection system (Applied Biosystems). The obtained data were normalized against the expression levels of mouse 18S recombinant RNA. The sequences of primer pairs were designed using Primer3 plus and are described in Table S1.

FACS analysis. Hearts were perfused with PBS and digested with collagenase. The infiltrated leukocytes in the digested supernatants were blocked with anti–mouse CD16/32 antibody (2.4G2; BD) for 5 min and then stained with antibodies to either FITC-conjugated anti–mouse CD45 (30-F11; eBioscience), PE-conjugated anti–mouse Gr-1 (RB6–8C5; BD), APC-conjugated anti–mouse F4/80 (BM8; eBioscience), or Pacific Blue–conjugated anti–mouse CD11b (M1/70; BioLegend) for 20 min. Cells were analyzed for composition using FACS Aria 2 (BD) with data analyzed by Flow Jo (Tree Star Inc.).

Measurements of fatty acids by GC–MS. Lipids were extracted by the method of Bligh and Dyer (Bligh and Dyer, 1959). Isolated phospholipids were methylated with 2.5% H_2SO_4 in methanol, and then the fatty acid methyl esters were extracted with hexane and subjected to gas chromatography-mass spectrometry (GC–MS) analysis. GC–MS analysis was performed by using an Agilent 7890A-5975C GC–MS network system (Agilent Technologies) equipped with a DB-23 capillary column (60 m × 250 μm × 0.15 μm; Agilent Technologies). The oven temperature program was as follows: an initial temperature of 50°C held for 1 min was raised to 175°C at 25°C/min, and then to 235°C at 5°C/min, and held for 5 min. The injector and detector temperatures were both set at 250°C.

Mediator lipidomics. LC-MS/MS–based lipidomics analyses were performed using a high-performance liquid chromatography (HPLC) system (Waters UPLC) with a linear ion-trap quadrupole mass spectrometer (QTRAP5500; AB SCIEX) equipped with an Acquity UPLC BEH C_{18} column (Waters) as described previously (Arita, 2012). MS/MS analyses were conducted in negative-ion mode, and fatty acid metabolites were identified and quantified by multiple reaction monitoring (MRM).

Statistical analysis. Values are presented as mean ± SEM. Comparisons between groups were made using a Mann-Whitney U test, whereas data among multiple groups were compared using the Kruskal-Wallis test with Bonferroni post-hoc testing. P < 0.05 was considered statistically significant. Statistical analysis was performed with SPSS 22.0 for Windows (SPSS, Inc.).

REFERENCES

Arita, M. 2012. Mediator lipidomics in acute inflammation and resolution. *J. Biochem.* 152:313–319. http://dx.doi.org/10.1093/jb/mvs092

Bligh, E.G., and W.J. Dyer. 1959. A rapid method of total lipid extraction and purification. *Can. J. Biochem. Physiol.* 37:911–917. http://dx.doi.org/10.1139/o59-099

Chen, J., G.C. Shearer, Q. Chen, C.L. Healy, A.J. Beyer, V.B. Nareddy, A.M. Gerdes, W.S. Harris, T.D. O'Connell, and D. Wang. 2011. Omega-3 fatty acids prevent pressure overload-induced cardiac fibrosis through activation of cyclic GMP/protein kinase G signaling in cardiac fibroblasts. *Circulation.* 123:584–593. http://dx.doi.org/10.1161/CIRCULATIONAHA.110.971853

Duda, M.K., K.M. O'Shea, B. Lei, B.R. Barrows, A.M. Azimzadeh, T.E. McElfresh, B.D. Hoit, W.J. Kop, and W.C. Stanley. 2007. Dietary supplementation with ω-3 PUFA increases adiponectin and attenuates ventricular remodeling and dysfunction with pressure overload. *Cardiovasc. Res.* 76:303–310. http://dx.doi.org/10.1016/j.cardiores.2007.07.002

Endo, J., M. Sano, J. Fujita, K. Hayashida, S. Yuasa, N. Aoyama, Y. Takehara, O. Kato, S. Makino, S. Ogawa, and K. Fukuda. 2007. Bone marrow derived cells are involved in the pathogenesis of cardiac hypertrophy in response to pressure overload. *Circulation.* 116:1176–1184. http://dx.doi.org/10.1161/CIRCULATIONAHA.106.650903

Epelman, S., K.J. Lavine, A.E. Beaudin, D.K. Sojka, J.A. Carrero, B. Calderon, T. Brija, E.L. Gautier, S. Ivanov, A.T. Satpathy, et al. 2014. Embryonic and adult-derived resident cardiac macrophages are maintained through distinct mechanisms at steady state and during inflammation. *Immunity.* 40:91–104. http://dx.doi.org/10.1016/j.immuni.2013.11.019

Fritsche, K. 2006. Fatty acids as modulators of the immune response. *Annu. Rev. Nutr.* 26:45–73. http://dx.doi.org/10.1146/annurev.nutr.25.050304.092610

Huang, M.J., L. Wang, X.C. Zheng, Z.M. Zhang, B. Yan, T.Y. Chen, X.C. Bai, and D.D. Jin. 2012. Intra-articular lentivirus-mediated insertion of the fat-1 gene ameliorates osteoarthritis. *Med. Hypotheses.* 79:614–616. http://dx.doi.org/10.1016/j.mehy.2012.07.035

Hudert, C.A., K.H. Weylandt, Y. Lu, J. Wang, S. Hong, A. Dignass, C.N. Serhan, and J.X. Kang. 2006. Transgenic mice rich in endogenous omega-3 fatty acids are protected from colitis. *Proc. Natl. Acad. Sci. USA.* 103:11276–11281. http://dx.doi.org/10.1073/pnas.0601280103

Isobe, Y., M. Arita, R. Iwamoto, D. Urabe, H. Todoroki, K. Masuda, M. Inoue, and H. Arai. 2013. Stereochemical assignment and anti-inflammatory properties of the omega-3 lipid mediator resolvin E3. *J. Biochem.* 153:355–360. http://dx.doi.org/10.1093/jb/mvs151

Kai, H., T. Mori, K. Tokuda, N. Takayama, N. Tahara, K. Takemiya, H. Kudo, Y. Sugi, D. Fukui, H. Yasukawa, et al. 2006. Pressure overload-induced transient oxidative stress mediates perivascular inflammation and cardiac fibrosis through angiotensin II. *Hypertens. Res.* 29:711–718. http://dx.doi.org/10.1291/hypres.29.711

Kang, J.X., J. Wang, L. Wu, and Z.B. Kang. 2004. Transgenic mice: fat-1 mice convert n-6 to n-3 fatty acids. *Nature.* 427:504. http://dx.doi.org/10.1038/427504a

Kayama, Y., T. Minamino, H. Toko, M. Sakamoto, I. Shimizu, H. Takahashi, S. Okada, K. Tateno, J. Moriya, M. Yokoyama, et al. 2009. Cardiac 12/15 lipoxygenase-induced inflammation is involved in heart failure. *J. Exp. Med.* 206:1565–1574. http://dx.doi.org/10.1084/jem.20082596

Koyanagi, M., K. Egashira, S. Kitamoto, W. Ni, H. Shimokawa, M. Takeya, T. Yoshimura, and A. Takeshita. 2000. Role of monocyte chemoattractant protein-1 in cardiovascular remodeling induced by chronic blockade of nitric oxide synthesis. *Circulation.* 102:2243–2248. http://dx.doi.org/10.1161/01.CIR.102.18.2243

Kuwahara, F., H. Kai, K. Tokuda, M. Takeya, A. Takeshita, K. Egashira, and T. Imaizumi. 2004. Hypertensive myocardial fibrosis and diastolic dysfunction: another model of inflammation? *Hypertension.* 43:739–745. http://dx.doi.org/10.1161/01.HYP.0000118584.33350.7d

Leuschner, F., P.J. Rauch, T. Ueno, R. Gorbatov, B. Marinelli, W.W. Lee, P. Dutta, Y. Wei, C. Robbins, Y. Iwamoto, et al. 2012. Rapid monocyte kinetics in acute myocardial infarction are sustained by extramedullary monocytopoiesis. *J. Exp. Med.* 209:123–137. http://dx.doi.org/10.1084/jem.20111009

Ma, F., Y. Li, L. Jia, Y. Han, J. Cheng, H. Li, Y. Qi, and J. Du. 2012. Macrophage-stimulated cardiac fibroblast production of IL-6 is essential for TGFβ/Smad activation and cardiac fibrosis induced by angiotensin II. *PLoS ONE.* 7:e35144. http://dx.doi.org/10.1371/journal.pone.0035144

Meléndez, G.C., J.L. McLarty, S.P. Levick, Y. Du, J.S. Janicki, and G.L. Brower. 2010. Interleukin 6 mediates myocardial fibrosis, concentric hypertrophy, and diastolic dysfunction in rats. *Hypertension.* 56:225–231. http://dx.doi.org/10.1161/HYPERTENSIONAHA.109.148635

Mozaffarian, D., and J.H.Y. Wu. 2011. Omega-3 fatty acids and cardiovascular disease: effects on risk factors, molecular pathways, and clinical events. *J. Am. Coll. Cardiol.* 58:2047–2067. http://dx.doi.org/10.1016/j.jacc.2011.06.063

Nahrendorf, M., F.K. Swirski, E. Aikawa, L. Stangenberg, T. Wurdinger, J.-L. Figueiredo, P. Libby, R. Weissleder, and M.J. Pittet. 2007. The healing

myocardium sequentially mobilizes two monocyte subsets with divergent and complementary functions. *J. Exp. Med.* 204:3037–3047. http://dx.doi.org/10.1084/jem.20070885

Nicoletti, A., D. Heudes, C. Mandet, N. Hinglais, J. Bariety, and J.B. Michel. 1996. Inflammatory cells and myocardial fibrosis: spatial and temporal distribution in renovascular hypertensive rats. *Cardiovasc. Res.* 32:1096–1107. http://dx.doi.org/10.1016/S0008-6363(96)00158-7

Nodari, S., M. Triggiani, U. Campia, A. Manerba, G. Milesi, B.M. Cesana, M. Gheorghiade, and L. Dei Cas. 2011. Effects of n–3 polyunsaturated fatty acids on left ventricular function and functional capacity in patients with dilated cardiomyopathy. *J. Am. Coll. Cardiol.* 57:870–879. http://dx.doi.org/10.1016/j.jacc.2010.11.017

Ogawa, S., D. Urabe, Y. Yokokura, H. Arai, M. Arita, and M. Inoue. 2009. Total synthesis and bioactivity of resolvin E2. *Org. Lett.* 11:3602–3605. http://dx.doi.org/10.1021/ol901350g

Oh, D.Y., S. Talukdar, E.J. Bae, T. Imamura, H. Morinaga, W. Fan, P. Li, W.J. Lu, S.M. Watkins, and J.M. Olefsky. 2010. GPR120 is an omega–3 fatty acid receptor mediating potent anti-inflammatory and insulin-sensitizing effects. *Cell.* 142:687–698. http://dx.doi.org/10.1016/j.cell.2010.07.041

Opie, L.H., P.J. Commerford, B.J. Gersh, and M.A. Pfeffer. 2006. Controversies in ventricular remodelling. *Lancet.* 367:356–367. http://dx.doi.org/10.1016/S0140-6736(06)68074-4

Sano, M., K. Fukuda, H. Kodama, J. Pan, M. Saito, J. Matsuzaki, T. Takahashi, S. Makino, T. Kato, and S. Ogawa. 2000. Interleukin-6 family of cytokines mediate angiotensin II–induced cardiac hypertrophy in rodent cardiomyocytes. *J. Biol. Chem.* 275:29717–29723. http://dx.doi.org/10.1074/jbc.M003128200

Tavazzi, L., A.P. Maggioni, R. Marchioli, S. Barlera, M.G. Franzosi, R. Latini, D. Lucci, G.L. Nicolosi, M. Porcu, and G. Tognoni Gissi–HF Investigators. 2008. Effect of n–3 polyunsaturated fatty acids in patients with chronic heart failure (the GISSI-HF trial): a randomised, double-blind, placebo-controlled trial. *Lancet.* 372:1223–1230. http://dx.doi.org/10.1016/S0140-6736(08)61239-8

Wan, J.-B., L.-L. Huang, R. Rong, R. Tan, J. Wang, and J.X. Kang. 2010. Endogenously decreasing tissue n–6/n–3 fatty acid ratio reduces atherosclerotic lesions in apolipoprotein E-deficient mice by inhibiting systemic and vascular inflammation. *Arterioscler. Thromb. Vasc. Biol.* 30:2487–2494. http://dx.doi.org/10.1161/ATVBAHA.110.210054

Weber, K.T., Y. Sun, S.K. Bhattacharya, R.A. Ahokas, and I.C. Gerling. 2013. Myofibroblast-mediated mechanisms of pathological remodelling of the heart. *Nat. Rev. Cardiol.* 10:15–26. http://dx.doi.org/10.1038/nrcardio.2012.158

Weylandt, K.H., A. Nadolny, L. Kahlke, T. Köhnke, C. Schmöcker, J. Wang, G.Y. Lauwers, J.N. Glickman, and J.X. Kang. 2008. Reduction of inflammation and chronic tissue damage by omega–3 fatty acids in fat–1 transgenic mice with pancreatitis. *Biochim. Biophys. Acta.* 1782:634–641. http://dx.doi.org/10.1016/j.bbadis.2008.08.011

Weylandt, K.H., L.F. Krause, B. Gomolka, C.-Y. Chiu, S. Bilal, A. Nadolny, S.F. Waechter, A. Fischer, M. Rothe, and J.X. Kang. 2011. Suppressed liver tumorigenesis in fat–1 mice with elevated omega–3 fatty acids is associated with increased omega–3 derived lipid mediators and reduced TNF-α. *Carcinogenesis.* 32:897–903. http://dx.doi.org/10.1093/carcin/bgr049

White, P.J., M. Arita, R. Taguchi, J.X. Kang, and A. Marette. 2010. Transgenic restoration of long-chain n–3 fatty acids in insulin target tissues improves resolution capacity and alleviates obesity-linked inflammation and insulin resistance in high-fat-fed mice. *Diabetes.* 59:3066–3073. http://dx.doi.org/10.2337/db10-0054

Wynn, T.A., and T.R. Ramalingam. 2012. Mechanisms of fibrosis: therapeutic translation for fibrotic disease. *Nat. Med.* 18:1028–1040. http://dx.doi.org/10.1038/nm.2807

Xia, S., Y. Lu, J. Wang, C. He, S. Hong, C.N. Serhan, and J.X. Kang. 2006. Melanoma growth is reduced in fat–1 transgenic mice: impact of omega–6/omega–3 essential fatty acids. *Proc. Natl. Acad. Sci. USA.* 103:12499–12504. http://dx.doi.org/10.1073/pnas.0605394103

Yokoyama, M., H. Origasa, M. Matsuzaki, Y. Matsuzawa, Y. Saito, Y. Ishikawa, S. Oikawa, J. Sasaki, H. Hishida, H. Itakura, et al. Japan EPA lipid intervention study (JELIS) Investigators. 2007. Effects of eicosapentaenoic acid on major coronary events in hypercholesterolaemic patients (JELIS): a randomised open-label, blinded endpoint analysis. *Lancet.* 369:1090–1098. http://dx.doi.org/10.1016/S0140-6736(07)60527-3

Zhang, M.J., and M. Spite. 2012. Resolvins: anti-inflammatory and proresolving mediators derived from omega-3 polyunsaturated fatty acids. *Annu. Rev. Nutr.* 32:203–227. http://dx.doi.org/10.1146/annurev-nutr-071811-150726